Quantifying Three Decades of Artisanal and Small-scale Gold Mining Frontiers in the Guiana Shield (1995–2024)

Elmontaserbellah Ammar[1], Sean J. Glynn[1], Kerry Anne Kansinally[2], William Clemens[3], Emilius Richter[3], Matthew J. Struebig[1], Jake E. Bicknell[1]

[1] Durrell Institute for Conservation and Ecology (DICE), School of Natural Sciences, University of Kent, Canterbury, UK

[2] Conservation International Guyana, Georgetown, Guyana

[3] dida Datenschmiede GmbH, Berlin, 10827, Germany

Author for correspondence: ea588@kent.ac.uk

Abstract

Artisanal and Small-scale Gold Mining (ASGM) is a leading driver of tropical deforestation and forest degradation, yet its spatial and temporal dynamics remain largely underexplored. Here, we present a pan-regional, annual time-series analysis of ASGM expansion across rainforests of the Guiana Shield (Guyana, Suriname, and French Guiana) from 1995 to 2024. Using Landsat imagery, we trained a deep learning model to detect gold mining patterns, and we used this to map nearly three decades of ASGM activity. Our results reveal a 995% increase in mine count and a 1,411% increase in total mined area, from ~13,200 ha in 1995 to ~199,489 ha in 2024. Mean mine polygon size increased by 38%, with especially sharp rises in Suriname, suggesting a shift toward more intensive operations. We estimate ASGM-driven aboveground carbon losses of 30,933 Gg C across the region, highlighting its growing climate implications. Mining disproportionately impacted key ecosystems, overlapping with protected areas and Key Biodiversity Areas, particularly in French Guiana. These trends signal escalating pressure on one of the world's most intact tropical forest frontiers and underscore the need for coordinated regional responses to mitigate ASGM's environmental footprint. Our findings also demonstrate the power of deep learning for scalable, long-term monitoring of extractive pressures across biodiverse landscapes.

Keywords: gold mining; tropical ecology; deep learning; semantic segmentation; Landsat time series; U-Net; remote sensing; aboveground carbon loss; tropical forest degradation; biodiversity loss; Guiana Shield; Amazonia; land-use change; deforestation; mineral extraction; protected areas.

1. Introduction

Tropical forest biomes have experienced growing pressure from gold mining, particularly since the turn of the 21st century. Demand for metals, especially gold, but also precious, industrial, and "transition" metals, has surged, driven by population growth, infrastructure expansion, urbanisation, and the shift toward low-carbon energy technologies (e.g. renewable power, batteries). This has led to expansion in both industrial and artisanal mining, which causes not only direct habitat loss through forest clearance, but also indirect effects via roads, soil erosion, disturbance of hydrological regimes and river sediments, pollution (notably mercury in ASGM), and land-use change around mining frontiers (Aldous et al., 2024; Dethier et al., 2023; Ladewig et al., 2024).

While agriculture remains the dominant cause of tropical deforestation, mining's proportional contribution has been rising sharply in many places (Kalamandeen et al., 2018). A pantropical study found that between 2000-2019, industrial mining directly caused the loss of 3,264 km^2 of tropical forest, with 80% of that loss concentrated in just four countries: Indonesia, Brazil, Ghana and Suriname (Giljum et al., 2022). When looking only at the tropical forests of South America, ~1,680 km^2 of forest was estimated lost due to gold mining from 2001 to 2013 (Alvarez-Berríos & Mitchell Aide, 2015).

The Guiana Shield region of Northern South America covers 26% of the Amazon (1.3 million km^2 of Guyana, Suriname, French Guiana, Brazil, Venezuela and Columbia); the earth's most critical terrestrial biome, accounting for ~30% of global terrestrial productivity and harbouring ~25% of all known biodiversity (Groombridge & Jenkins, 2002; Malhi et al., 2006; Roy et al., 2001). Here, Artisanal and Small-scale Gold Mining (ASGM) is the primary driver of forest loss accounting for an estimated ~160,000 ha % within the Guyanas (Guyana, Suriname, and French Guiana) by the year 2014 (Rahm et al., 2021). This is important because the region is home to some of the highest levels of biodiversity and carbon in the world, and represents one of the planet's last remining wilderness areas (Bovolo et al., 2018; Funk et al., 2007;

Grenyer et al., 2006; Griscom et al., 2009; Hammond, 2005; Huber, 1995; Saatchi et al., 2011). Moreover the region is known for its pivotal role in regulating the climate of the wider Amazon basin by being the primary source area for atmospheric moisture that flows determines pan-continental weather (Bovolo et al., 2018). As such it is predicted that run-away deforestation in the Guiana Shield will lead to mass-die for parts of the Amazon, alongside more extreme dry seasons (Zemp et al., 2017).

Early work by the French National Forestry Office (ONF) using Landsat (30m), and SPOT (10-20m) imagery documented a tripling of deforestation indicators between 1999–2001 and 2007–2008, with forest loss in Suriname, French Guiana, and Guyana rising from a combined ~20,000 ha to more than 60,000 ha due to gold mining. Using MODIS (250m) data, Alvarez-Berríos & Mitchell Aide (2015) further estimated that ~68,400 ha of forest was lost to gold mining in the Guianan moist forest ecoregion between 2001 and 2013, representing 41% of all gold mining deforestation in the tropical and subtropical moist broadleaf forest biome. More recently, Rahm et al., (2021), drawing on Landsat, RapidEye (5m), and SPOT imagery, digitized a total of 160,850 ha of gold mining areas between 2012 and 2014, with roughly half of this deforestation in Guyana, 34% in Suriname, 15% in French Guiana, and 1% in Amapá.

A number of recent global-scale mining mapping studies have attempted to quantify mining activity worldwide (Liang et al., 2021; Maus et al., 2020, 2022; Tang & Werner, 2023). These studies provide valuable context for understanding global trends in mining but are known to underestimate ASGM. Several methodological factors contribute to this underestimation. Maus et al., (2020, 2022) relied on visual interpretation of satellite imagery within pre-defined buffers around known mine coordinates from the SNL Metals and Mining database, which were optimized to capture large, long-lived mines but frequently excluded small, diffuse artisanal operations characteristic of the Guiana Shield. Similarly, Liang et al., (2021) and Tang & Werner (2023) primarily delineated mining polygons from Google Earth and Sentinel-2 imagery, focusing on well-documented or formal mining operations,

often excluding fragmented, informal, or historically intermittent ASGM sites. Limitations inherent to these approaches include heterogeneous spatial resolution of imagery, temporal gaps in available data, and aggregation of multiple mining features into single generalized polygons. Consequently, small-scale mines, and tailing areas typical of ASGM are frequently omitted or misrepresented.

There is consequently a need for studies that can delineate mining operations and associated habitat loss, at the fine scale, to understand the true extent of this important driver of biodiversity and environmental breakdown. There is also the need for consistent, long-term monitoring of ASGM expansion across tropical forests, and the Guiana Shield represents a suitable test bed to undertake such research. As such, this is now possible due to advances in remote sensing and machine learning to detect and track mining activity across large spatial and temporal scales with increasing accuracy (Barenblitt et al., 2021; Camalan et al., 2022; Isidro et al., 2017; Nava et al., 2022; Nyamekye et al., 2021; Swenson et al., 2011). Remote sensing has become the primary means of detecting and quantifying ASGM across tropical forests. Optical imagery has been widely used to delineate mine areas, but its effectiveness can be limited by persistent cloud cover and spectral confusion with other forms of bare soil (Barenblitt et al., 2021; Nava et al., 2022). Radar data, which can penetrate clouds, has been applied less frequently but offers unique advantages for monitoring mining disturbances in persistently cloudy regions (Ballère et al., 2021; Forkuor et al., 2020). A range of methodological approaches have been developed, from traditional statistical classifiers to machine learning and deep learning algorithms, each with different strengths depending on image resolution, spectral bands, and landscape context (Asner et al., 2013; Elmes et al., 2014; Nyamekye et al., 2021). While these studies demonstrate that ASGM can be mapped with moderate to high accuracy, most have been restricted to specific sites or short time windows, leaving open the challenge of consistently characterising ASGM expansion over multiple decades.

In this study, we present the first large scale time series analysis of ASGM growth spanning nearly three decades (1995–2024). We undertake this work in the Guiana

Shield, drawing on Landsat satellite imagery and a deep learning semantic segmentation model trained to identify gold mining footprints. This study aimed to: 1. Evaluate the effectiveness of applying a deep learning approach to detect and monitor ASGM from Landsat imagery, assessing its utility for long-term, regional-scale monitoring; 2. Quantify the temporal expansion of ASGM across the Guiana Shield region from 1995 to 2024, including changes in the number, size, and total area of mines; 3. Compare national-level trends in ASGM growth in Guyana, Suriname, and French Guiana, exploring differences in the pace, scale, and intensity of mining activity; 4. Estimate the aboveground carbon (AGC) loss attributable to ASGM between 2000 and 2024, using spatially explicit forest biomass data and country-specific mine footprints; 5. Assess the spatial footprint of mining relative to each country's total land area and forest cover, to contextualize the broader landscape-level impacts; 6. Evaluate the overlap between ASGM and areas of high conservation value, including designated protected areas and Key Biodiversity Areas (KBAs), to inform conservation priorities and land-use planning. Together, these provide a regional-scale, longitudinal assessment of ASGM's environmental footprint, with implications for forest conservation, carbon emissions accounting, and policy interventions across the Guiana Shield.

2. Methods

2.1. Study Region and Study Area

Our study focuses on three countries within the Guiana Shield: Guyana, Suriname, and French Guiana (an overseas territory of France) (Figure 1). These countries share the same moist tropical rainforest (MTR) biome, characterized by a mean annual temperature above 25 °C at sea level and persistently high cloud cover. Cloud density is particularly intense in the western portion of the study area (Guyana) and becomes less pronounced towards the east (French Guiana). The region experiences two rainy seasons annually: a longer wet season from May to August and a shorter one from December to January.

To delineate our initial study region, we first reviewed all Landsat path/row tiles covering the political boundaries of the three countries in 2024 to identify where ASGM activity was visible. From this initial set of tiles, we then limited our analysis to those tiles where ASGM activity was visibly observable, based on the spectral and spatial patterns of mining activity (e.g. tailings and pits) in 2024 Landsat imagery. We assume that, if these areas had no observable mining in 2024, that they likely never had mining activity, since even abandoned ASGM sites leave behind characteristic scars of vegetated tailings and pits decades later. These tiles were further refined using QGIS to exclude areas dominated by Cerrado savanna and urban land cover, focusing the analysis strictly on rainforest-dominated landscapes. The final study area (highlighted in orange in Figure 1) therefore represents rainforest areas in Guyana, Suriname, and French Guiana where mining activity was visually observed from Landsat imagery in 2024. These study region-limiting steps were taken to make the processing of hundreds of large satellite images more manageable, and less computationally expensive.

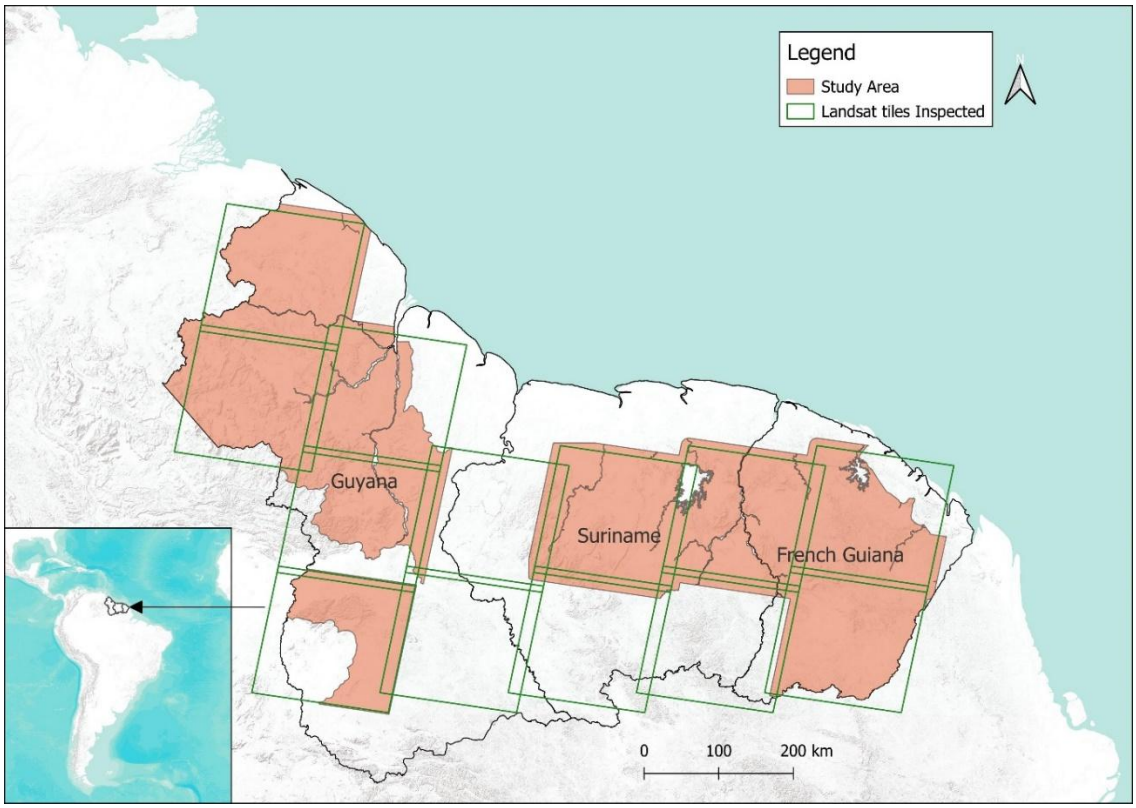

Figure 1: Satellite tiles inspected (green outlines), and the final study area (highlighted in orange) spanning parts of Guyana, Suriname, and French Guiana within the Guiana Shield.

2.2. Satellite Imagery

To detect mining using remote sensing, we employed imagery from the Landsat Satellite program, specifically using Landsat 5 TM (1995–2011), Landsat 8 OLI (2013–present), and Landsat 9 OLI (2021–present). Landsat 7 ETM+ was excluded due to scan-line corrector failure (Storey et al., 2005) which introduces data gaps. We used Collection 2, Level 2, Tier-1 surface reflectance products, selecting the Red, Green, Blue (RGB), Near-Infrared (NIR), Infrared (IR), Shortwave Infrared-1 (SWIR-1), and Shortwave Infrared-2 (SWIR-2) bands. These spectral bands are effective for distinguishing forest from non-forest cover and for identifying exposed soil and bare ground, typical features of ASGM sites (Asner et al., 2013; Barenblitt et al., 2021; Camalan et al., 2022; Elmes et al., 2014; Nyamekye et al., 2021).

All available scenes from 1995 to 2024 were downloaded for the selected tiles within our study region (outlined in section 2.1; paragraph 2). Scenes with severe atmospheric distortion or residual sensor artifacts were filtered out to retain only high-quality imagery.

2.3. Deep Learning Training and Inference

Reviewing every satellite image manually over nearly 30 years of Landsat data would not be feasible, given the vast number of images (~ 700 Landsat scenes), each covering an area of 185 × 185 km (~34,000 km^2). To overcome this challenge, we developed an automated deep learning workflow to detect gold mining activity across the Guiana Shield. The workflow automatically scanned each image, identified areas with visual signatures of mining, and generated polygons that trace around the boundary of each detected site. This approach allowed us to consistently and efficiently map mining activity across space and time, something that would be prohibitively time and labour intensive using manual interpretation and digitization alone.

To do this we used a convolutional neural network model, ‘ASMSpotter’, to detect ASGM activity. ASMSpotter is a U-Net-based (Ronneberger et al., 2015) deep

learning segmentation tool developed by Dida machine learning (GmbH, 2025) to support segmentation of heterogeneous mining patterns from satellite imagery. The model was originally developed for use with Sentinel-2 imagery; however, we re-trained it for Landsat use by using a set of ~500 manually drawn ASGM binary training masks (see examples of 'hand-labelled training masks' in Figure S1) derived from visual interpretation of Landsat composites and very high-resolution reference imagery (e.g. Google Earth). Training masks were drawn only for areas where mining features such as tailings, pits, and access roads were clearly visible, ensuring high confidence in boundary placement. These training masks captured a range of mining typologies; active, abandoned, clustered and dispersed, across different landscape contexts, but all within the tropical rainforest biome.

To evaluate model performance on an independent test set, we used the F1 metric; a standard performance metric that balances precision (the proportion of predicted mines that were correct) and recall (the proportion of actual mines that were detected). The formulas used to calculate precision, recall, and F1, respectively are:

$$Precision = \frac{True\ Positives}{True\ Positives + False\ Positives}$$

$$Recall = \frac{True\ Positives}{True\ Positives + False\ Negatives}$$

$$F1 = 2 \times \frac{Precision \times Recall}{Precision + Recall}$$

To enhance model performance, we expanded our Landsat training dataset through a form of manual data augmentation. The original training set consisted of 500 manually drawn ASGM masks created for this study. To increase dataset diversity and model generalization, we duplicated these 500 masks and re-edited them using a slightly different labelling style that applied smoother, more generalized boundaries. This produced a total of 1,000 varied training samples, exposing the model to both precise and generalized representations of mine shapes. The model initialized with pre-trained Sentinel-2 model weights but was fully retrained using this Landsat-based dataset, which substantially improved performance on test

data. To verify the efficacy of this approach, we compared F1 scores across 10 independent tests between (i) dataset 1, the doubled dataset using both labelling styles (S2), and (ii) dataset 2, the original dataset with each image appearing once and without labelling variation (S2). Dataset 1 showed a significantly higher median F1 score than dataset 2 ($t(18) = 20$; $p < 0.0001$). Based on this result, dataset 1 was used in subsequent analyses to improve model performance.

To make the model more robust to differences in image orientation and reduce overfitting, we trained it using a range of image flips and rotations (Shorten & Khoshgoftaar, 2019). This technique helps the model recognize mining patterns regardless of how they appear in the scene. Each training sample was a 256 x 256 (at 30 m spatial resolution per pixel) pixel image patch that combined three spectral band layers: near-infrared reflectance (NIR), the Normalized Difference Vegetation Index (NDVI), and the Bare Soil Index (BSI). All inputs were normalized so that pixel values were comparable across scenes. The model was trained to minimize a "dice loss" function (Tilborghs et al., 2022), which helps balance the difference between mining and non-mining areas and improves boundary accuracy. Training was optimized using the Adam algorithm (Kingma & Ba, 2017), with automatic stopping once performance stopped improving (see S4 for loss plot). 788 tiles were used for training and 196 tiles for validation. During testing, the model achieved an F1 score of 0.855, with a precision of 0.849 and recall of 0.861 (i.e. the model successfully delineated gold mines ~85% of the time).

All multi-band GeoTIFF rasters (excluding the Ultraviolet (UV) band from OLI sensors) were input into the trained ASMSpotter model for inference. Model inference was performed in Python using the PyTorch framework, with raster handling and feature extraction implemented through the Rasterio library and vector outputs exported as GeoJSON using the geojson package. To address cloud cover, predictions from all available images within a given year (~23 images per year) be up to were merged into a single layer, ensuring that areas obscured in one acquisition were complemented by detections from cloud-free observations. Post-

processed binary masks were subsequently vectorized into polygon shapefiles delineating predicted ASGM areas.

2.4. Temporal Range

The study covers the period 1995–2024. We chose 1995 as the baseline year after reviewing earlier Landsat-5 imagery (available from 1984) to identify when spatially clustered ASGM activity first became clearly visible. We did not conduct formal analyses before 1995. The earliest persistent cluster of mines in our study area was located in central Guyana, while comparable clusters in Suriname and French Guiana only began to emerge after 2000. Starting in 1995 therefore allowed us to capture nearly three decades of ASGM expansion across the Guiana Shield.

2.5. Area Calculations

The output polygons (i.e. detected mines) from ASMSpotter were imported into QGIS for spatial analysis. For each year, the area of individual polygons was computed and summarized to yield annual statistics, including total ASGM area, mean polygon size, median area, and interquartile range. These metrics provide a basis for evaluating both the extent and typical configuration of ASGM activity over time.

2.6. AGC Lost Calculations

To quantify potential carbon losses driven by ASGM, Aboveground Biomass (AGB) statistics were derived from the 2000 aboveground biomass dataset provided by Harris et al. (2021). Since this dataset reflects biomass values as of the year 2000, we constrained our Aboveground Carbon (AGC) loss estimates to the period 2000–2024. Although our dataset included mining activity from 1995 onward, we could not quantify the associated biomass loss prior to 2000 due to the lack of AGB baseline data for earlier years. As such, AGC loss values represent post-2000 forest carbon loss attributable to gold mining.

To estimate AGC loss from forests due to ASGM activity, we applied a biomass-to-carbon conversion approach based on our annual predicted mining extents

described above. For the year 2024, we multiplied the total mined area (in hectares) by the median AGB per hectare for the Guiana Shield rainforest biome. The resulting biomass value was then multiplied by a conversion factor of 0.47 (reflecting the proportion of biomass that is carbon) (Goslee et al., 2016) and converted from megagrams (Mg) to gigagrams (Gg) by dividing by 1000. The general formula used to calculate the midpoint estimate (AGC loss median) is:

$$AGC_{loss}(Gg) = Area_{mined} \times AGB_{per\ ha}(Mg/ha) \times \left(\frac{0.47}{1000}\right)$$

Where: $AGC_{loss}(Gg)$ is the aboveground carbon lost in gigagrams, $Area_{mined}$ is the annual sum of predicted ASGM area in hectares, $AGB_{per\ ha}(Mg/ha)$ is the median aboveground biomass in megagrams per hectare, 0.47 is the standard biomass-to-carbon conversion factor for tropical forests, and 1000 is used to convert the final carbon estimate from megagrams to gigagrams.

To provide an estimate of uncertainty in AGC loss, we repeated this calculation using the lower quartile (Q1) and upper quartile (Q3) values of AGB per hectare, also derived from the same source. This yielded two additional AGC loss estimates: $AGC_{loss}(Gg)\min$ (using Q1 AGB), and $AGC_{loss}(Gg)\max$ (using Q3 AGB).

3. Results

3.1. Temporal Growth of ASGM (1995–2024)

Across the Guiana Shield, gold mining activity increased over the 29-year study period (Figure 2A-B). The cumulative area affected by mining expanded from 13,200 ha in 1995 to 199,489 ha in 2024, a 1,411% relative increase in total mapped mine area (Figure 3A; S5). The mean size of mine polygons also grew over time, reflecting the expansion of individual mining sites (Figure 3B). Finally, the total number of mapped mine polygons rose from 1,235 in 1995 to 13,503 in 2024, a 995% relative increase (Figure 3C; S5).

This expansion did not occur at a constant rate. Between 1995 and 2005, the number of mines grew steadily from 1,235 to 4,083, and the affected area rose relatively by 312%, from 13,200 ha to 54,394 ha. During the 2005–2015-decade,

growth accelerated further, reaching 9,164 mines and 144,710 ha of impacted area by 2015, a 166% relative increase in area over ten years. In the final period (2015–2024), mining continued to expand, though at a slightly slower pace, rising to 13,503 mines and 199,489 ha by 2024, equivalent to a 38% relative increase in area over the last decade (Figure 3; S5).

Spatially, ASGM hotspots were concentrated in northwest and central Guyana (Figure 2), particularly along river networks, and in mid-eastern Suriname around the Brokopondo Reservoir (Figure 2). In French Guiana, activity was most prominent in a horizontal central band (Figure 2).

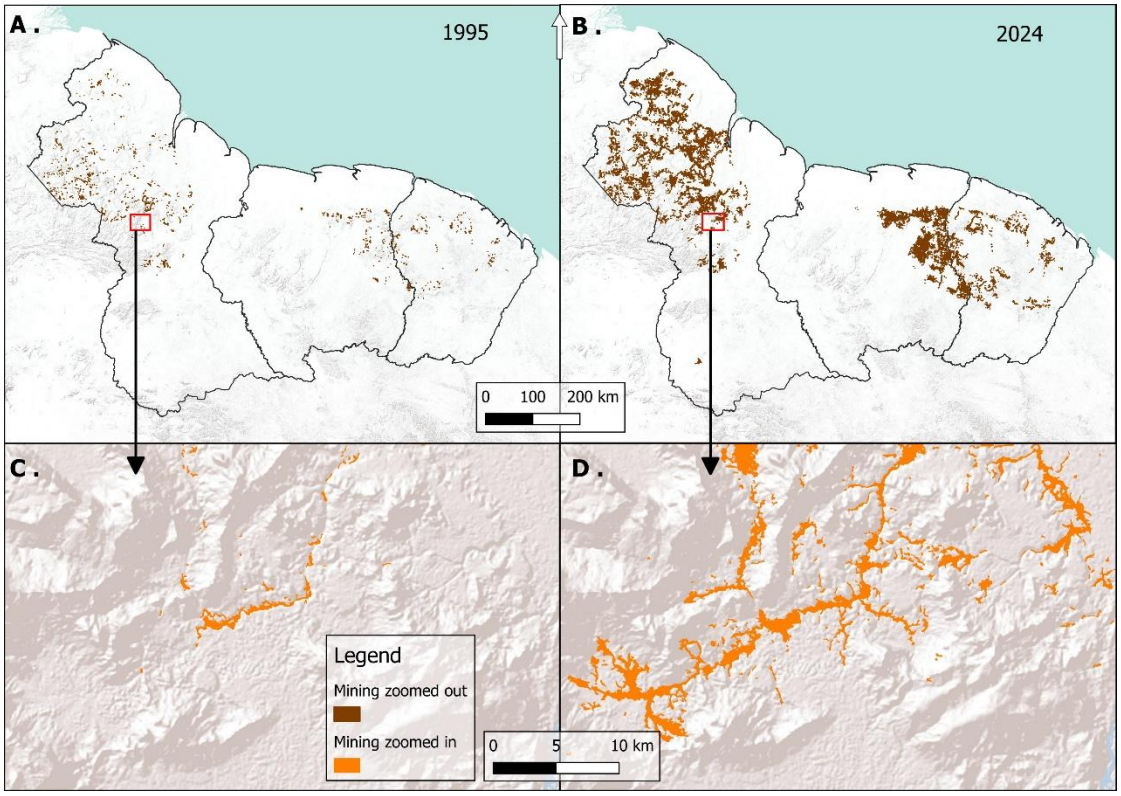

Figure 2: Predicted gold mining polygons (brown) across the Guiana Shield in 1995 (A) and 2024 (B), highlighting the substantial increase in mined area. Panels C (1995) and D (2024) show a zoomed-in view of central Guyana, illustrating local expansion of mining activity (orange) over the same period.

3.2. National-level trends

In Guyana, gold mining activity increased substantially across all three decades. In 1995, a total of 782 mining areas were detected, covering 10,131 ha at an average

size of 12.96 ha. By 2005, mine count had more than doubled to 1,659, and total mine area had risen to 21,389 ha, a 111% relative increase (Figure 4A–C; S6). Between 2005 and 2015, mine extent expanded further, with 5,764 mining polygons mapped over 78,100 ha, representing a 265% relative increase in area. From 2015 to 2024, the upward trend continued, though at a slower rate, reaching 8,175 polygons covering 118,832 ha, a 52% relative increase. Mean mine polygon size in Guyana remained relatively stable, fluctuating between 13 and 18 ha and peaking at 18.14 ha in 2022 (Figure 4A–C; S6).

In Suriname, increases were most pronounced in terms of relative expansion and mean mine polygon size. In 1995, 244 mines were mapped, affecting 1,479 ha (mean size 6.06 ha). By 2005, mine count had risen to 1,274 and impacted area to 19,500 ha, a 1,219% relative increase (Figure 4D–F; S7). From 2005 to 2015, the number of mines reached 2,101, covering 55,874 ha (+186%). During the final period, 2015–2024, expansion accelerated further, with 3,149 mines covering 68,712 ha by 2024. Mean mine polygon size increased sharply from 6.1 ha in 1995 to 21.8 ha in 2024, with peaks above 30 ha in 2022 and 2023 (Figure 4D–F; S7).

French Guiana showed a slower trajectory. In 1995, 209 mines were identified, affecting 1,590 ha (mean size 7.61 ha). By 2005, mine count rose to 1,150 and area to 13,505 ha, a 750% relative increase (Figure 4G–I; S8). From 2005 to 2015, activity stabilised, with 1,299 mines and a reduced total area of 10,736 ha. After 2015, expansion resumed, with a surge in 2023–2024 leading to 2,179 mines covering 11,946 ha by 2024. Mean mine polygon size declined over time, reaching 5.48 ha (Figure 4G–I; S8).

Taken together, Guyana had the largest overall areal extent of mining by 2024, while Suriname exhibited the steepest proportional increases in both area and mean mine polygon size. French Guiana, in contrast, experienced the slowest expansion, with smaller mines dominating throughout the study period.

3.3. Changes in mean mine polygon size

Mean mine polygon size increased over time across the region, though this trend varied by country. For the entire study area, mean mine polygon size rose from 10.69 ha in 1995 to 14.77 ha in 2024, a 38% relative increase (Figure 3B; S5). In Guyana, mean mine polygon size fluctuated but remained within the 12–18 ha range, reflecting a mix of persistent small-scale and emerging medium-scale operations (Figure 4B; S6). In Suriname, however, mean mine polygon size increased steeply from 6.1 ha in 1995 to a peak of 32.8 ha in 2023, before slightly declining to 21.8 ha in 2024, suggesting both intensification and consolidation of mining activities (Figure 4E; S7). French Guiana, on the other hand, saw relatively modest changes, with mean mine polygon size remaining under 10 ha for most years and declining to 5.5 ha in 2024 (Figure 4H; S8).

3.4. Aboveground Carbon Loss

Estimates of aboveground carbon (AGC) loss attributable to ASGM from 2000 to 2024 reveal significant carbon impacts across all three countries in the study area (Table 1 & Table 2). Total AGC lost by 2024 due to mining activity was highest in Guyana, with a median estimate of 16,859 Gg C (range: 14,639–18,275 Gg C), reflecting both greater mined area and higher interquartile variation in AGB (IQR = 65 Mg/ha). In Suriname, the median AGC loss was 11,980 Gg C (range: 10,979–12,408 Gg C), with the narrower range corresponding to lower spatial variability in forest biomass (IQR = 38 Mg/ha). French Guiana had the lowest total AGC loss, with a median estimate of 2,094.35 Gg C, ranging from 1,933.33 Gg C to 2,174.11 Gg C. Despite having the highest AGB per hectare, its comparatively low AGC loss reflects the more limited spatial extent of detected ASGM activity over the study period.

3.5. Mining Area as a Proportion of Country Area, Forest Cover, Protected Areas, and KBAs

Across the Guiana Shield, the spatial footprint of ASGM varied substantially among countries when expressed as a percentage of total land area and forest cover (Figure 5B-C). In Guyana, the summed mining area represented 0.56% of the country's total land area, while in Suriname and French Guiana, mining accounted for 0.47% and 0.14% of land area, respectively. When considering only forest

biomes, the proportional impact was higher: mining areas comprised 0.67% of Guyana's forest cover, 0.53% in Suriname, and 0.15% in French Guiana.

The proportion of mining activity occurring within protected areas and Key Biodiversity Areas (KBAs) also differed by country (Figure 6). In Guyana, 0.78% of the total mapped mining area overlapped with protected areas, while in Suriname and French Guiana, the corresponding values were 1.15% and 26.25%, respectively. For KBAs, the percentage of mining area falling within these priority conservation zones was 0.41% in Guyana, 7.90% in Suriname, and 8.57% in French Guiana (Figure 6 insets).

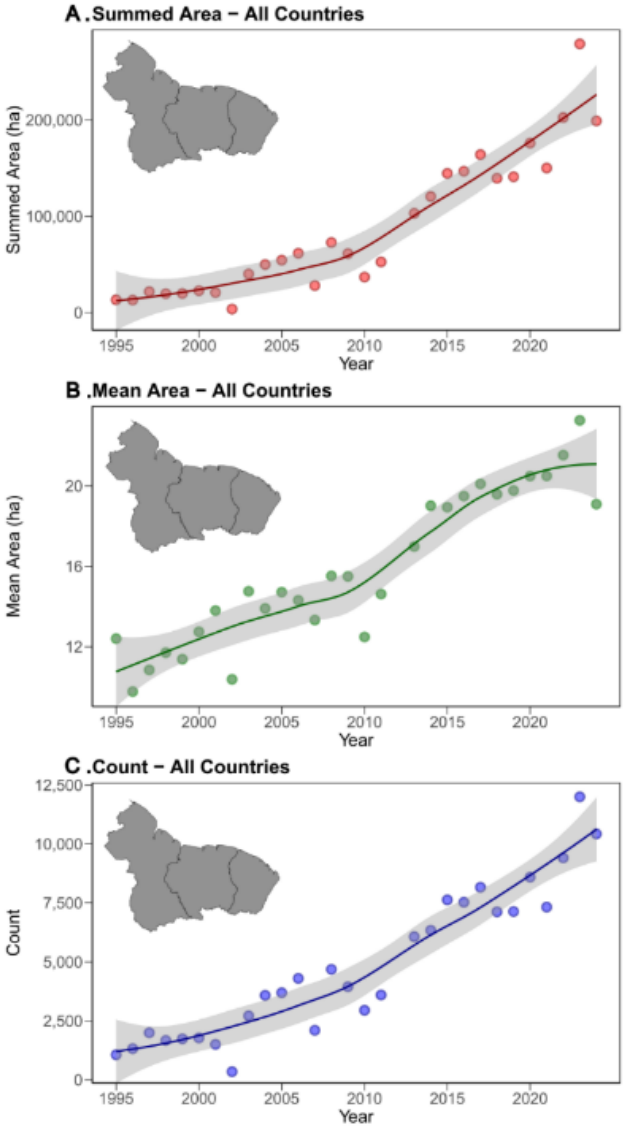

Figure 3: Scatterplot (**A**) shows summed predicted gold mine polygon areas (ha) per year on the Y axis and years passed (from the baseline year of 1995 to the end year of 2024) on the X axis. Scatterplot (**B**) shows the count of predicted gold mine polygons per year on the Y axis and years passed (from the baseline year of 1995 to the end year of 2024) on the X axis. Scatterplot (**C**) shows the mean area (ha) of predicted gold mine polygon areas (ha) per year on the Y axis and years passed (from the baseline year of 1995 to the end year of 2024) on the X axis. Trend line shading uses locally estimated scatterplot smoothing (loess) with 95% CI shown by grey shading.

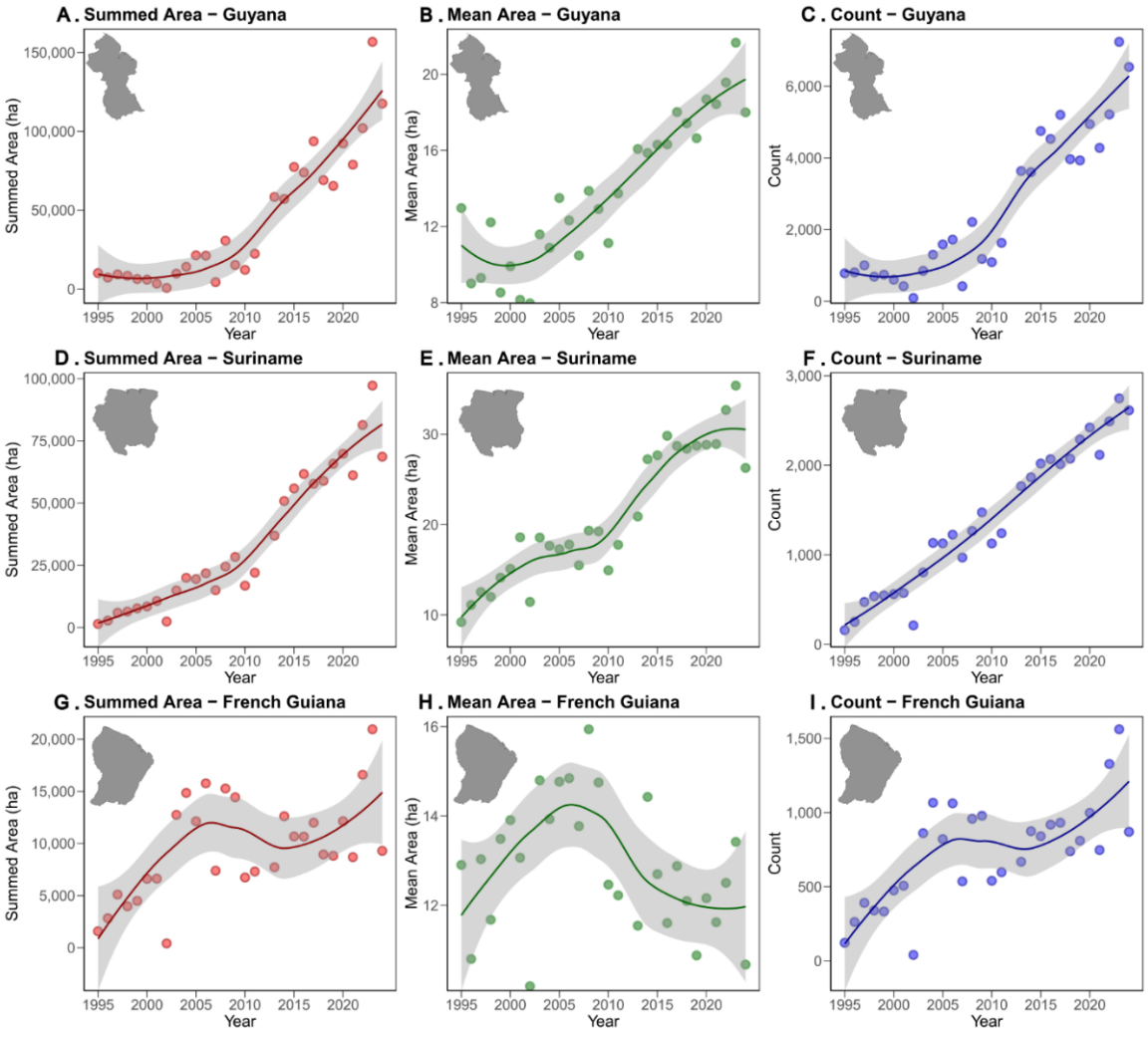

Figure 4: Scatterplot (A,D,G) shows summed predicted mine polygon areas (ha) per year on the Y axis and years passed (from the baseline year of 1995 to the end year of 2024) on the X axis. Scatterplot (B,E,H) shows the count of predicted mine polygons per year on the Y axis and years passed (from the baseline year of 1995 to

the end year of 2024) on the X axis. Scatterplot (C,F,I) shows the mean area (ha) of predicted mine polygon areas (ha) per year on the Y axis and years passed (from the baseline year of 1995 to the end year of 2024) on the X axis. Trend line shading uses locally estimated scatterplot smoothing (loess) with 95% CI shown by grey shading.

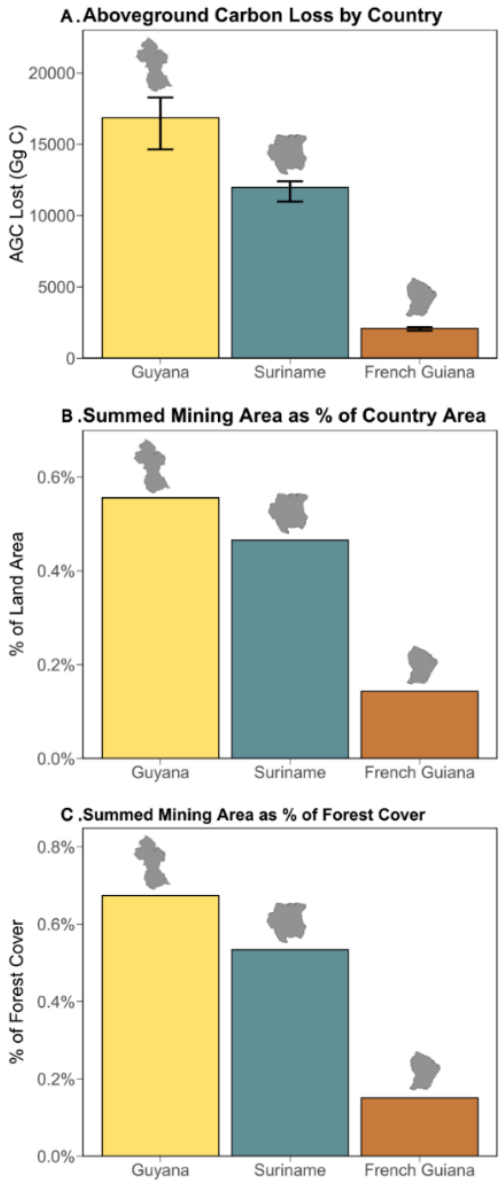

Figure 5: (A) Estimated aboveground carbon (AGC) loss and mining area impacts due to ASGM activity across the Guiana Shield region from 2000 to 2024. Bars represent median AGC loss (in gigagrams of carbon, Gg C) per country. Error bars denote lower and upper bound estimates based on the 25th and 75th percentile AGB values, respectively (AGB data from Harris et al., 2021). (B) Summed mining area as a percentage of each country's total land area. (C) Summed mining area as a percentage of each country's total forest cover.

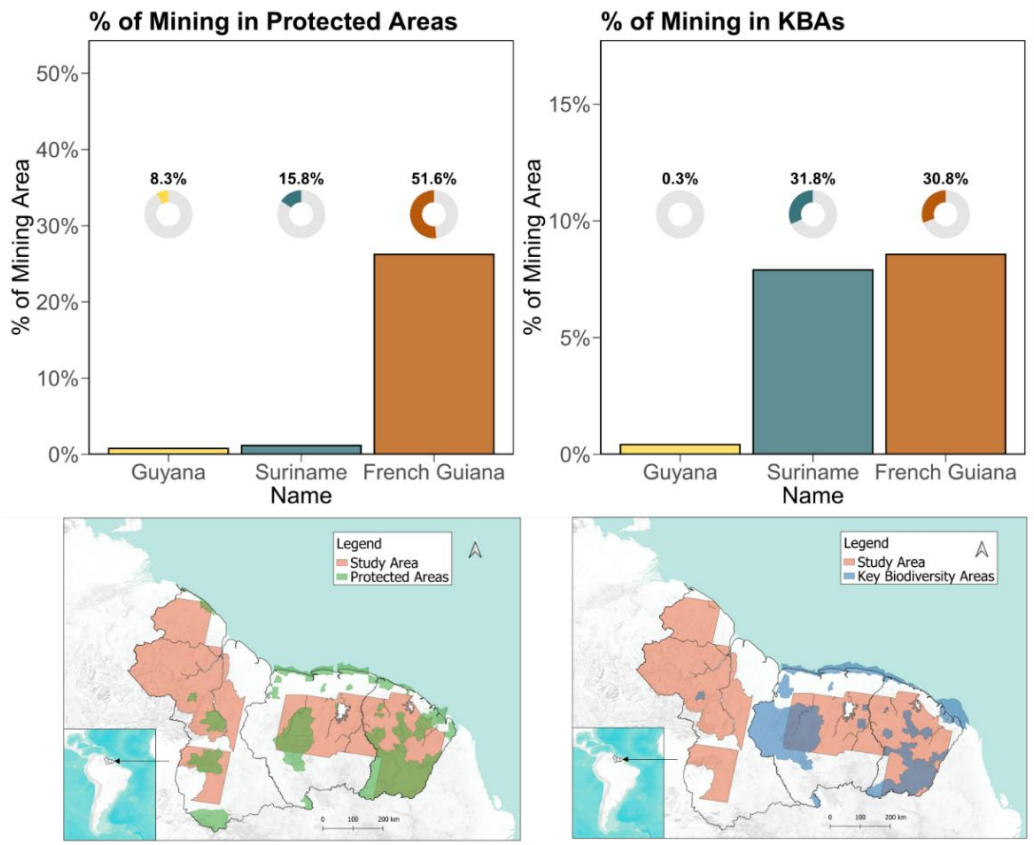

Figure 6: Proportion of total mining area occurring within protected areas in the final year of the dataset - 2024 (UNEP-WCMC and IUCN, 2025) (top left), and Key Biodiversity Areas (KBAs) (top right) for each country in the Guiana Shield. Bars show the percentage of each country's total ASGM area that falls within designated protected areas or KBAs based on spatial overlays of mining and conservation boundaries. Above each bar, a donut chart illustrates the percentage of that country's total land area that is covered by protected areas or KBAs, with the exact value shown above each donut. The map in the bottom left shows protected area coverage overlayed onto the study area, and the map in the bottom right shows KBAs overlayed with the study area.

Table 1: Table shows lower quartile AGB p/ha (in the year 2000), median AGB p/ha (in the year 2000), upper quartile AGB p/ha, interquartile range AGB p/ha, and AGC (Gg C) lost (minimum, median, and maximum estimates with a conversion factor of 0.47) by 2024 for each of the three countries in the study area.

Country	Q1 AGB	Q2 AGB	Q3 AGB	Median (min-max) – Gg AGC
Guyana	262	302	327	16,859 (14,639 - 18,275)
Suriname	340	371	378	11,980 (10,979 - 12,408)
French Guiana	344	373	387	2,094 (1,933 - 2,174)

4. Discussion

4.1. Regional Expansion of ASGM and Ecological Impacts

Our findings reveal a sharp and sustained expansion of ASGM across rainforest regions of the Guiana Shield over the last three decades. The 733% increase in mapped mine count and 1,163% increase in total mined area between 1995 and 2024 underscore the intensifying pressure that ASGM exerts on tropical forest ecosystems in this region (Alvarez-Berríos & Mitchell Aide, 2015; Dezécache et al., 2017; Hayes et al., 2023; Rahm et al., 2021). As ASGM operations extend into previously undisturbed forest cores, they fragment large tracts of habitat, triggering cascading biodiversity impacts through, habitat loss, and species displacement (Glynn et al., 2025; Stoll et al., 2022) . These effects are compounded by indirect consequences, including sedimentation of river systems, mercury contamination, and reductions in forest regeneration potential (Dethier et al., 2023; Kalamandeen et al., 2020; Rahm et al., 2021; Roopnarine, 2006). The increase in mean mine polygon size from 13 ha in 1995 to 20 ha in 2024 suggests a shift toward more intensive operations with greater potential for environmental degradation per unit area.

4.2. Divergent National Trajectories in Mining Growth

Despite the regional trend of ASGM expansion, the extent and spatial distribution of mining activity varied among countries. Guyana exhibited the highest proportion of land and forest affected by mining, with 0.56% of its total land area and 0.67% of its forest cover impacted. Suriname followed closely, with 0.47% of land area and 0.53% of forest cover affected. In contrast, French Guiana showed the lowest

proportional mining footprint, with only 0.14% of land area and 0.15% of forest cover impacted, these trends are consistent with those documented in Rahm et al., (2021).

In addition to differences in proportional land and forest cover affected, countries exhibited different trajectories in the absolute number of mines, total mined area, and average mine size over time. Guyana experienced the largest absolute expansion in all three metrics. In Guyana, the expansion of ASGM primarily involved a growing number of mines rather than larger individual sites, suggesting persistence of small- and medium-scale operations. Suriname exhibited both rapid proliferation and intensification of ASGM, with emerging larger-scale operations over time. French Guiana experienced slower growth in both the number and size of mine polygons compared to its neighbours. The decreasing trend in all three metrics seen in French Guiana between the early 2000's and mid to late 2010's seems to correspond with the law enforcement's crackdown on illegal mining in French Guiana, which began in the early 2000's (Dezécache et al., 2017; MacDonald, 2016). It is also notable that mean mine polygon size showed a general decrease from the mid 2000's onwards, unlike mine count, and summed mine area which began rising again experiencing after the mid 2000's dip. This may point to a shift towards smaller scale discrete operations in order to avoid detection, however further research would be needed to confirm this.

4.3. Methodological Considerations: Resolution and Dataset Limitations

Suriname's emergence of larger-scale operations may help explain the findings of Alvarez-Berríos & Mitchell Aide (2015). Using coarse-resolution imagery (250 m), they reported that Suriname contained the majority of gold-mining-related deforestation in the Guianan moist forest ecoregion. However, both our results and those of Rahm et al., (2021), which rely on finer-resolution imagery (5–30 m), identify Guyana as the most impacted country. More broadly, these discrepancies illustrate a limitation of both coarse-resolution regional studies and global-scale mining datasets (Liang et al., 2021; Maus et al., 2020, 2022; Tang & Werner, 2023). By focusing on large, well-documented mines or formal operations, and using

coarse imagery, studies frequently miss the small, diffuse, and fragmented mines that dominate ASGM in the Guiana Shield. Consequently, the relative impacts among countries may appear distorted, particularly for regions like Guyana where small-scale mines are pervasive. These considerations highlight the importance of using fine-resolution, temporally consistent imagery and regionally tailored mapping approaches to capture the true extent and dynamics of ASGM. Without such methods, assessments risk underestimating mining footprints, mischaracterising national trajectories, and overlooking the cumulative impacts of small but widespread operations that drive much of the environmental change in the Guiana Shield.

4.4. Conservation Implications: Overlap with Protected Areas and Key Biodiversity Areas

The spatial overlap between ASGM and conservation zones also differed among countries. In French Guiana, 26.25% of the total mapped mining area overlapped with protected areas, substantially higher than in Suriname and Guyana. Similarly, the proportion of ASGM activity occurring within Key Biodiversity Areas (KBAs) was highest in French Guiana, followed by Suriname, and Guyana. These findings highlight that, although the overall mining footprint in French Guiana is comparatively small, its location disproportionately affects areas of high conservation value. These patterns are consistent with Rahm et al., (2021), who also reported that French Guiana's protected areas were the most impacted by mining across the Guiana Shield, with over 4,000 ha of mining-related deforestation inside PAs compared to minimal impacts in Suriname and Guyana. Our analysis complements this by showing that French Guiana's mines not only overlap protected areas but also disproportionately fall within KBAs, extending the conservation implications beyond statutory reserves.

At the broader Amazonian scale, Alvarez-Berríos & Mitchell Aide (2015) found that gold mining frequently overlaps protected lands, especially multiple-use zones, and causes substantial forest loss within 10 km of PA boundaries. Our results, and the findings of previous studies show that mining pressures in Amazonia often

concentrate in and around biodiversity priority areas, threatening both formally designated reserves and adjacent landscapes.

4.5. Socio-Economic Drivers of ASGM Expansion

Several overlapping socio-economic drivers likely underpin the observed expansion of ASGM over the study period. First, recurring gold price booms, particularly after 2005, have made informal mining an increasingly attractive livelihood option to people with limited alternative income sources (Dezécache et al., 2017; Hammond et al., 2007). Second, weak environmental enforcement and limited institutional capacity in remote forested areas have allowed ASGM to proliferate relatively unchecked (MacDonald, 2016; Roopnarine, 2006), especially in transboundary zones. Third, continued international demand for gold fuels a persistent incentive structure for growth (*Gold Spot Price and Cost of Gold*, 2025).

4.6. Carbon Consequences of ASGM Across the Guiana Shield

The spatial expansion of ASGM has driven substantial potential aboveground carbon (AGC) loss across the Guiana Shield, with important implications for regional carbon stocks and climate mitigation. Carbon impacts were particularly pronounced in Guyana and Suriname, where mining concentrated in high-biomass forest areas, leading to disproportionately large losses. By contrast, French Guiana's smaller ASGM footprint helped limit overall AGC loss despite its high per-hectare biomass. The wider uncertainty range in Guyana's AGC estimates (~3,600 Gg C) reflects greater heterogeneity in mined landscapes and underscores the need for tailored restoration and monitoring strategies. These findings are especially relevant in the context of REDD+ frameworks and other mechanisms aimed at preserving carbon stocks (Government of Guyana, 2022; Government of Suriname, 2019). While ASGM is often framed around habitat loss and pollution, (Asner et al., 2013; Dethier et al., 2023; Glynn et al., 2025; Rahm et al., 2021; Stoll et al., 2022), its contribution to carbon emissions through deforestation and forest degradation demands greater attention in both climate and conservation policy (e.g. Hayes et al., 2023).

4.7. Limitations and Future Research Needs

While this study provides the most extensive time-series assessment of ASGM expansion in the Guiana Shield to date, our deep learning model is not without limitations. The ASMSpotter model achieved an F1 score of 0.855, so some false positives and false negatives are expected. In particular, rivers, roads, and savannah areas are occasionally misclassified as mining. We are aware of these errors and have made every effort to minimise their impact by manually reviewing outputs and removing false positives wherever possible.

Taken together, these findings offer strong evidence that ASGM is a major and driver of ecological and carbon loss across the Guiana Shield. Compared to other regions of the Amazon, the rate of mine expansion and associated carbon loss in the Guiana Shield is similarly rapid, though the absolute area affected remains smaller than hotspots such as the Madre de Dios region in Peru (Asner et al., 2013; Swenson et al., 2011). Across the broader tropics, ASGM-induced forest degradation remains a key but often overlooked driver of carbon emissions, emphasizing the need for spatially explicit monitoring beyond traditional deforestation metrics. As global demand for gold persists, effective mitigation will require integrated approaches that couple improved monitoring with restoration efforts. Future research should evaluate the long-term ecological consequences of ASGM expansion for biodiversity, water systems, and forest regeneration.

5. Conclusion

Our study provides the first pan-regional, multi-decadal analysis of ASGM expansion in the Guiana Shield. By applying a deep learning model to nearly 30 years of Landsat imagery, we reveal a dramatic 1,411% relative increase in mined area and a near tenfold rise in mine numbers since 1995. This expansion has driven significant aboveground carbon losses and intensified pressures on forests of exceptional biodiversity and global climate importance. National trajectories diverged: Guyana sustained the largest total mining extent, Suriname showed the steepest proportional growth and shift toward larger operations, while French

Guiana experienced slower expansion but higher overlap with protected areas and KBAs. These patterns highlight how ASGM impacts differ across governance and landscape contexts. Importantly, our findings demonstrate that global mining datasets have underestimated ASGM in the Guiana Shield, underscoring the necessity of regionally focused, high-resolution monitoring. Given the Shield's role in biodiversity conservation, carbon storage, and climate regulation, managing the impacts of ASGM expansion is essential. Integrating remote sensing with targeted policy interventions can better anticipate pressures on mining frontiers, and support strategies that minimise environmental harm in one of the world's most intact tropical forest regions.

Data Accessibility

Processed annual mining maps and code used for analysis will be made available upon publication of the peer-reviewed article.

Conflicts of Interest Statement

The authors declare no conflicts of interest.

Author Contributions Statement

Elmontaserbellah Ammar: Conceptualization, methodology, formal analysis, investigation, data curation, visualizations (lead), writing – original draft, writing – review and editing. Sean J. Glynn: Regional expertise, writing – review and editing. Kerry Anne Kansinally: Regional expertise, writing – review and editing. Emilius Richter: Software, model development. William Clemens: Software, model development. Matthew J. Struebig: Conceptual guidance, writing – review and editing. Jake E. Bicknell: Conceptual guidance, methodology, visualizations, writing – review and editing.

Acknowledgements

We thank colleagues at the Durrell Institute for Conservation and Ecology (DICE) for valuable discussion and feedback throughout this project. We are grateful to

partners at Dida Datenschmiede GmbH for technical collaboration on model development. We also thank Conservation International Guyana for insights into regional mining dynamics.

References

Aldous, A. R., Tear, T., & Fernandez, L. E. (2024). The global challenge of reducing mercury contamination from artisanal and small-scale gold mining (ASGM): Evaluating solutions using generic theories of change. *Ecotoxicology*, *33*(4), 506–517. https://doi.org/10.1007/s10646-024-02741-3

Alvarez-Berríos, N. L., & Mitchell Aide, T. (2015). Global demand for gold is another threat for tropical forests. *Environmental Research Letters*, *10*(1), 014006. https://doi.org/10.1088/1748-9326/10/1/014006

Asner, G. P., Llactayo, W., Tupayachi, R., & Luna, E. R. (2013). Elevated rates of gold mining in the Amazon revealed through high-resolution monitoring. *Proceedings of the National Academy of Sciences*, *110*(46), 18454–18459. https://doi.org/10.1073/pnas.1318271110

Ballère, M., Bouvet, A., Mermoz, S., Le Toan, T., Koleck, T., Bedeau, C., André, M., Forestier, E., Frison, P., & Lardeux, C. (2021). SAR data for tropical forest disturbance alerts in French Guiana: Benefit over optical imagery. *REMOTE SENSING OF ENVIRONMENT*, *252*. https://doi.org/10.1016/j.rse.2020.112159

Barenblitt, A., Payton, A., Lagomasino, D., Fatoyinbo, L., Asare, K., Aidoo, K., Pigott, H., Som, C., Smeets, L., Seidu, O., & Wood, D. (2021). The large footprint of small-scale artisanal gold mining in Ghana. *SCIENCE OF THE TOTAL ENVIRONMENT*, *781*. https://doi.org/10.1016/j.scitotenv.2021.146644

Bovolo, C. I., Wagner, T., Parkin, G., Hein-Griggs, D., Pereira, R., & Jones, R. (2018). The Guiana Shield rainforests—Overlooked guardians of South American climate. *Environmental Research Letters*, *13*(7), 074029. https://doi.org/10.1088/1748-9326/aacf60

Caballero Espejo, J., Messinger, M., Román-Dañobeytia, F., Ascorra, C., Fernandez, L. E., & Silman, M. (2018). Deforestation and Forest Degradation Due to Gold

689 Mining in the Peruvian Amazon: A 34-Year Perspective. *Remote Sensing*,
690 *10*(12), 1903. https://doi.org/10.3390/rs10121903
691 Camalan, S., Cui, K., Pauca, V., Alqahtani, S., Silman, M., Chan, R., Plemmons, R.,
692 Dethier, E., Fernandez, L., & Lutz, D. (2022). Change Detection of Amazonian
693 Alluvial Gold Mining Using Deep Learning and Sentinel-2 Imagery. *REMOTE*
694 *SENSING*, *14*(7). https://doi.org/10.3390/rs14071746
695 Dethier, E. N., Silman, M., Leiva, J. D., Alqahtani, S., Fernandez, L. E., Pauca, P.,
696 Çamalan, S., Tomhave, P., Magilligan, F. J., Renshaw, C. E., & Lutz, D. A.
697 (2023). A global rise in alluvial mining increases sediment load in tropical
698 rivers. *Nature*, *620*(7975), 787–793. https://doi.org/10.1038/s41586-023-
699 06309-9
700 Dezécache, C., Faure, E., Gond, V., Salles, J.-M., Vieilledent, G., & Hérault, B. (2017).
701 Gold-rush in a forested El Dorado: Deforestation leakages and the need for
702 regional cooperation. *Environmental Research Letters*, *12*(3), 034013.
703 https://doi.org/10.1088/1748-9326/aa6082
704 Earth Science Data Systems, N. (2025). *NASADEM Merged DEM Global 1 arc*
705 *second V001* | *NASA Earthdata* [Dataset]. Earth Science Data Systems,
706 NASA. https://www.earthdata.nasa.gov/data/catalog/lpcloud-nasadem-hgt-
707 001
708 Elmes, A., Yarlequé Ipanaqué, J. G., Rogan, J., Cuba, N., & Bebbington, A. (2014).
709 Mapping licit and illicit mining activity in the Madre de Dios region of Peru.
710 *Remote Sensing Letters*, *5*(10), 882–891.
711 Forkuor, G., Ullmann, T., & Griesbeck, M. (2020). Mapping and Monitoring Small-
712 Scale Mining Activities in Ghana using Sentinel-1 Time Series (2015-2019).
713 *REMOTE SENSING*, *12*(6). https://doi.org/10.3390/rs12060911
714 Funk, V., Hollowell, T., Berry, P., Kelloff, C., & Alexander, S. (2007). *Checklist of the*
715 *Plants of the Guiana Shield (Venezuela: Amazonas, Bolivar, Delta Amacuro;*
716 *Guyana, Surinam, French Guiana, Smithsonian Institution Volume 55: 1-*
717 *584)*.
718 Giljum, S., Maus, V., Kuschnig, N., Luckeneder, S., Tost, M., Sonter, L. J., &
719 Bebbington, A. J. (2022). A pantropical assessment of deforestation caused

by industrial mining. *Proceedings of the National Academy of Sciences*, *119*(38), e2118273119. https://doi.org/10.1073/pnas.2118273119

Glynn, S. J., Struebig, M. J., O'Shea, B. J., Allicock, B., Herce, J., Hall, L., Harris, A. E., Davies, Z. G., & Bicknell, J. E. (2025). Understorey bird responses to the abandonment of artisanal gold mining in Guyana. *Journal of Applied Ecology*, *n/a*(n/a). https://doi.org/10.1111/1365-2664.70148

GmbH, dida D. (2025). *ASMSpotter Demo: Detecting Artisanal Mining Activity Using AI*. https://dida.do/demos/asmspotter

Gold Spot Price and Cost of Gold. (2025, September 25). World Gold Council. https://www.gold.org/goldhub/data/gold-prices

Goslee, K., Walker, S. M., Grais, A., Murray, L., Casarim, F., & Brown, S. (2016). Module C-CS: calculations for estimating carbon stocks. *LEAF Technical Guidance Series for the Development of a Forest Carbon Monitoring System for REDD*.

Government of Guyana. (2022, July). *Guyana's Low Carbon Development Strategy 2030*. Office of the President, Government of Guyana. https://www.lcds.gov.gy

Government of Suriname. (2019). *National REDD+ Strategy of Suriname*. National Institute for Environment and Development in Suriname (NIMOS). https://www.surinameredd.org

Grenyer, R., Orme, C. D. L., Jackson, S. F., Thomas, G. H., Davies, R. G., Davies, T. J., Jones, K. E., Olson, V. A., Ridgely, R. S., Rasmussen, P. C., Ding, T.-S., Bennett, P. M., Blackburn, T. M., Gaston, K. J., Gittleman, J. L., & Owens, I. P. F. (2006). Global distribution and conservation of rare and threatened vertebrates. *Nature*, *444*(7115), 93–96. https://doi.org/10.1038/nature05237

Griscom, B., Shoch, D., Stanley, B., Cortez, R., & Virgilio, N. (2009). Sensitivity of amounts and distribution of tropical forest carbon credits depending on baseline rules. *Environmental Science & Policy*, *12*(7), 897–911. https://doi.org/10.1016/j.envsci.2009.07.008

Groombridge, B., & Jenkins, M. (2002). *World atlas of biodiversity: Earth's living resources in the 21st century*. Univ of California Press.

751 Hammond, D. S. (2005). *Tropical forests of the Guiana shield: Ancient forests in a*
752 *modern world*. CABI.
753 Hammond, D. S., Gond, V., Thoisy, B. de, Forget, P.-M., & DeDijn, B. P. E. (2007).
754 Causes and Consequences of a Tropical Forest Gold Rush in the Guiana
755 Shield, South America. *AMBIO: A Journal of the Human Environment*, *36*(8),
756 661–670. https://doi.org/10.1579/0044-7447(2007)36[661:CACOAT]2.0.CO;2
757 Hayes, W. M., Voigt, M., Rosa, I., Cort, K. A., Kotlinski, N., Kalamandeen, M., Davies,
758 Z. G., & Bicknell, J. E. (2023). Predicting the loss of forests, carbon stocks
759 and biodiversity driven by a neotropical 'gold rush'. *Biological Conservation*,
760 *286*, 110312. https://doi.org/10.1016/j.biocon.2023.110312
761 Huber, O. (1995). Geographical and physical features. *Flora of the Venezuelan*
762 *Guayana*, *1*, 1–61.
763 Isidro, C., McIntyre, N., Lechner, A., & Callow, I. (2017). Applicability of Earth
764 Observation for Identifying Small-Scale Mining Footprints in a Wet Tropical
765 Region. *REMOTE SENSING*, *9*(9). https://doi.org/10.3390/rs9090945
766 Kalamandeen, M., Gloor, E., Johnson, I., Agard, S., Katow, M., Vanbrooke, A.,
767 Ashley, D., Batterman, S. A., Ziv, G., Holder-Collins, K., & others. (2020).
768 Limited biomass recovery from gold mining in Amazonian forests. *Journal of*
769 *Applied Ecology*, *57*(9), 1730–1740.
770 Kalamandeen, M., Gloor, E., Mitchard, E., Quincey, D., Ziv, G., Spracklen, D.,
771 Spracklen, B., Adami, M., Aragão, L. E. O. C., & Galbraith, D. (2018). Pervasive
772 Rise of Small-scale Deforestation in Amazonia. *Scientific Reports*, *8*(1), 1600.
773 https://doi.org/10.1038/s41598-018-19358-2
774 Kingma, D. P., & Ba, J. (2017). *Adam: A Method for Stochastic Optimization*
775 (arXiv:1412.6980). arXiv. https://doi.org/10.48550/arXiv.1412.6980
776 Ladewig, M., Angelsen, A., Masolele, R. N., & Chervier, C. (2024). Deforestation
777 triggered by artisanal mining in eastern Democratic Republic of the Congo.
778 *Nature Sustainability*, *7*(11), 1452–1460. https://doi.org/10.1038/s41893-024-
779 01421-8
780 Liang, T., Werner, T. T., Heping, X., Jingsong, Y., & Zeming, S. (2021). A global-scale
781 spatial assessment and geodatabase of mine areas. *Global and Planetary*
782 *Change*, *204*, 103578. https://doi.org/10.1016/j.gloplacha.2021.103578

MacDonald, K. (2016). The Geopolitics of Gold in Northern Amazonia. *The Extractive Industries and Society*, *3*(3), 659–668. https://doi.org/10.1016/j.exis.2016.02.012

Malhi, Y., Wood, D., Baker, T. R., Wright, J., Phillips, O. L., Cochrane, T., Meir, P., Chave, J., Almeida, S., Arroyo, L., Higuchi, N., Killeen, T. J., Laurance, S. G., Laurance, W. F., Lewis, S. L., Monteagudo, A., Neill, D. A., Vargas, P. N., Pitman, N. C. A., … Vinceti, B. (2006). The regional variation of aboveground live biomass in old-growth Amazonian forests. *Global Change Biology*, *12*(7), 1107–1138. https://doi.org/10.1111/j.1365-2486.2006.01120.x

Maus, V., Giljum, S., da Silva, D. M., Gutschlhofer, J., da Rosa, R. P., Luckeneder, S., Gass, S. L. B., Lieber, M., & McCallum, I. (2022). An update on global mining land use. *Scientific Data*, *9*(1), 433. https://doi.org/10.1038/s41597-022-01547-4

Maus, V., Giljum, S., Gutschlhofer, J., da Silva, D. M., Probst, M., Gass, S. L. B., Luckeneder, S., Lieber, M., & McCallum, I. (2020). A global-scale data set of mining areas. *Scientific Data*, *7*(1), 289. https://doi.org/10.1038/s41597-020-00624-w

Nava, L., Cuevas, M., Meena, S., Catani, F., & Monserrat, O. (2022). Artisanal and Small-Scale Mine Detection in Semi-Desertic Areas by Improved U-Net. *IEEE GEOSCIENCE AND REMOTE SENSING LETTERS*, *19*. https://doi.org/10.1109/LGRS.2022.3220487

Nyamekye, C., Ghansah, B., Agyapong, E., & Kwofie, S. (2021). Mapping changes in artisanal and small-scale mining (asm) landscape using machine and deep learning algorithms.-a proxy evaluation of the 2017 ban on asm in ghana. *Environmental Challenges*, *3*, 100053.

Rahm, M., Smartt, T., Paloeng, C., Kasanpawiro, C., Moe Soe Let, V., Pichot, C., Bedeau, C., Farias, P., Carvalho, R., & Villien, C. (2021). Monitoring the impact of gold mining on the forest cover and freshwater in the Guiana Shield. *Reference Year*, *60*, pp40.

Ronneberger, O., Fischer, P., & Brox, T. (2015). *U-Net: Convolutional Networks for Biomedical Image Segmentation* (arXiv:1505.04597). arXiv. https://doi.org/10.48550/arXiv.1505.04597

Roopnarine, L. (2006). Small-Scale Gold Mining and Environmental Policy Challenges in Guyana: Protection or Pollution. *Canadian Journal of Latin American and Caribbean Studies / Revue Canadienne Des Études Latino-Américaines et Caraïbes*, *31*(61), 115–143.

Roy, J., Saugier, B., & Mooney, H. A. (2001). *Terrestrial global productivity*. Academic Press.

Saatchi, S. S., Harris, N. L., Brown, S., Lefsky, M., Mitchard, E. T., Salas, W., Zutta, B. R., Buermann, W., Lewis, S. L., Hagen, S., & others. (2011). Benchmark map of forest carbon stocks in tropical regions across three continents. *Proceedings of the National Academy of Sciences*, *108*(24), 9899–9904.

Shorten, C., & Khoshgoftaar, T. M. (2019). A survey on Image Data Augmentation for Deep Learning. *Journal of Big Data*, *6*(1), 60. https://doi.org/10.1186/s40537-019-0197-0

Stoll, E., Roopsind, A., Maharaj, G., Velazco, S., & Caughlin, T. T. (2022). Detecting gold mining impacts on insect biodiversity in a tropical mining frontier with SmallSat imagery. *Remote Sensing in Ecology and Conservation*.

Storey, J. C., Scaramuzza, P., Schmidt, G. L., & Barsi, J. (2005). *Landsat 7 scan line corrector-off gap-filled product development*. William T. Pecora Memorial Symposium on Remote Sensing, 16th. https://pubs.usgs.gov/publication/70259127?utm_source=chatgpt.com

Swenson, J., Carter, C., Domec, J., & Delgado, C. (2011). Gold Mining in the Peruvian Amazon: Global Prices, Deforestation, and Mercury Imports. *PLOS ONE*, *6*(4). https://doi.org/10.1371/journal.pone.0018875

Tang, L., & Werner, T. T. (2023). Global mining footprint mapped from high-resolution satellite imagery. *Communications Earth & Environment*, *4*(1), 134. https://doi.org/10.1038/s43247-023-00805-6

Tilborghs, S., Bertels, J., Robben, D., Vandermeulen, D., & Maes, F. (2022). The dice loss in the context of missing or empty labels: Introducing Φ and ϵ. *International Conference on Medical Image Computing and Computer-Assisted Intervention*, 527–537.

Zemp, D. C., Schleussner, C.-F., Barbosa, H. M. J., Hirota, M., Montade, V., Sampaio, G., Staal, A., Wang-Erlandsson, L., & Rammig, A. (2017). Self-amplified

Amazon forest loss due to vegetation-atmosphere feedbacks. *Nature Communications*, *8*(1), 14681. https://doi.org/10.1038/ncomms14681

UNEP-WCMC and IUCN (2025) Protected Planet: The World Database on Protected Areas (WDPA), 06/2025, Cambridge, UK: UNEP-WCMC and IUCN. Available at: www.protectedplanet.net.

Supplementary Materials

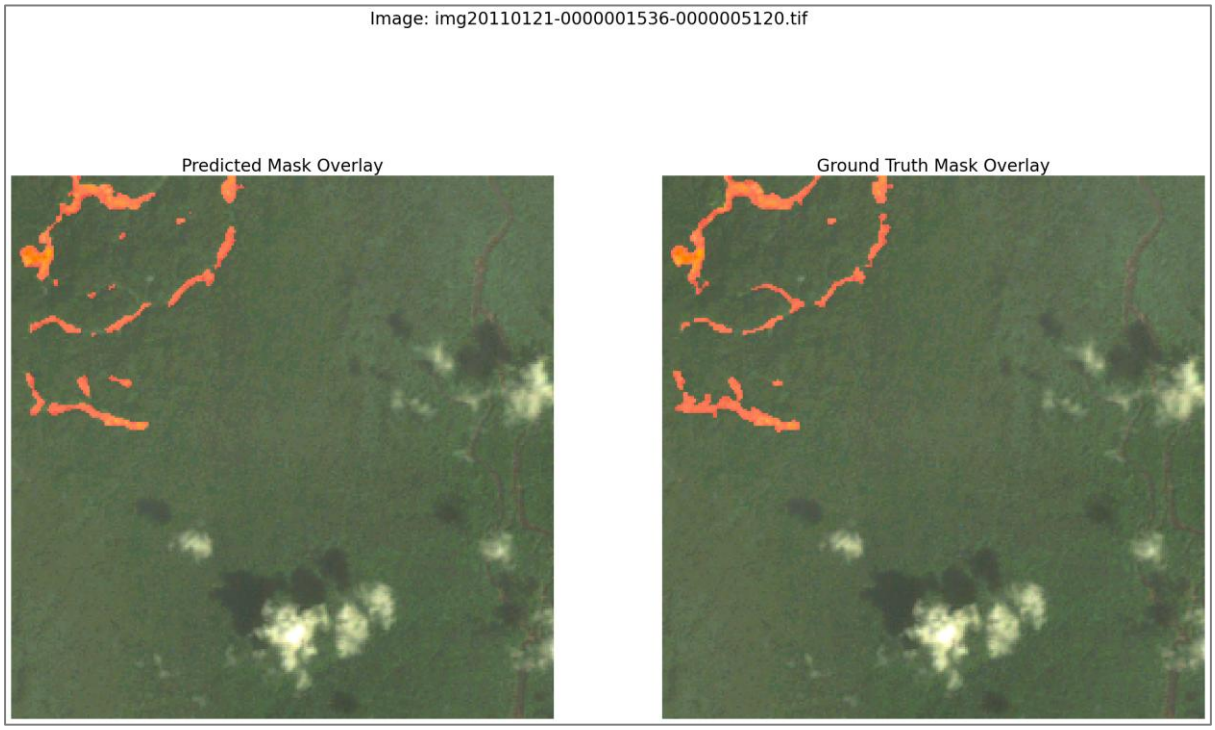

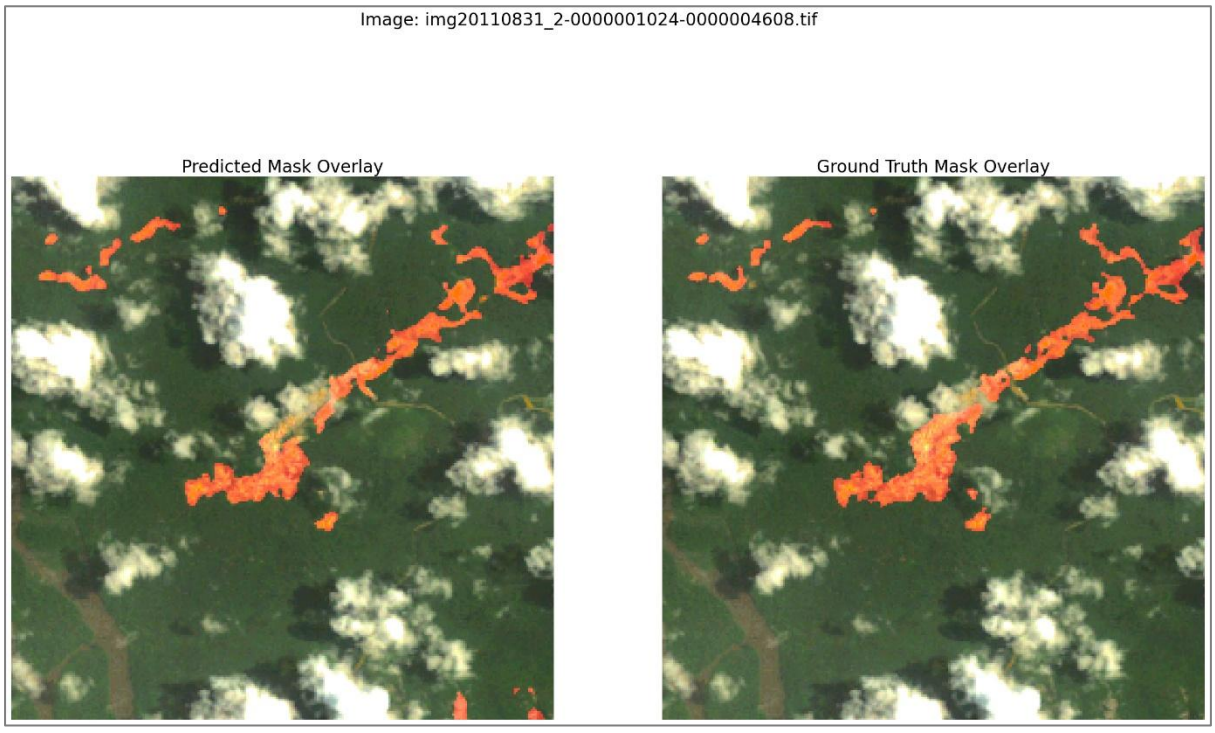


Image: img20231015-0000005632-0000001792.tif
Predicted Mask Overlay
Ground Truth Mask Overlay

855

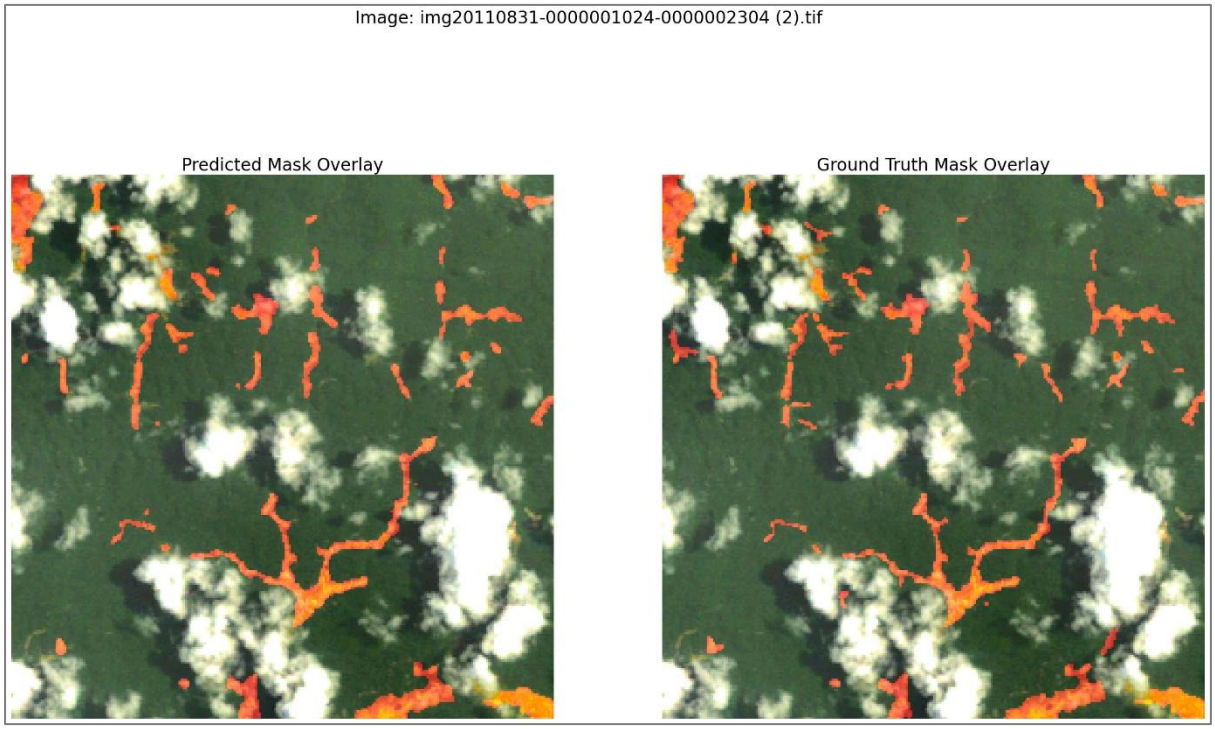
Image: img20110831-0000001024-0000002304 (2).tif
Predicted Mask Overlay
Ground Truth Mask Overlay

856

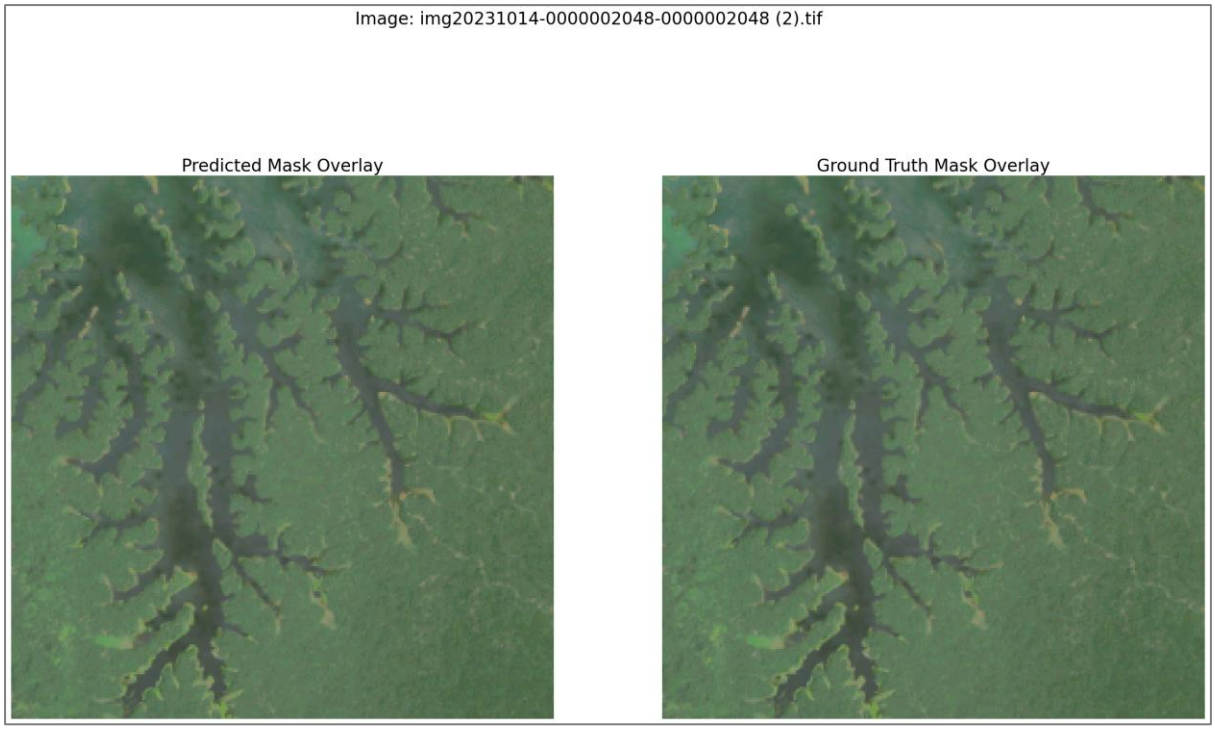

Figure **S1:** Five examples out of thirty hold-out 256 x 256 (30m pixel) tiles from a test-set showing our ASMSpotter model predictions alongside hand-digitized labels, illustrating performance on unseen Landsat tiles containing a mixture of ASGM and non-ASGM areas.

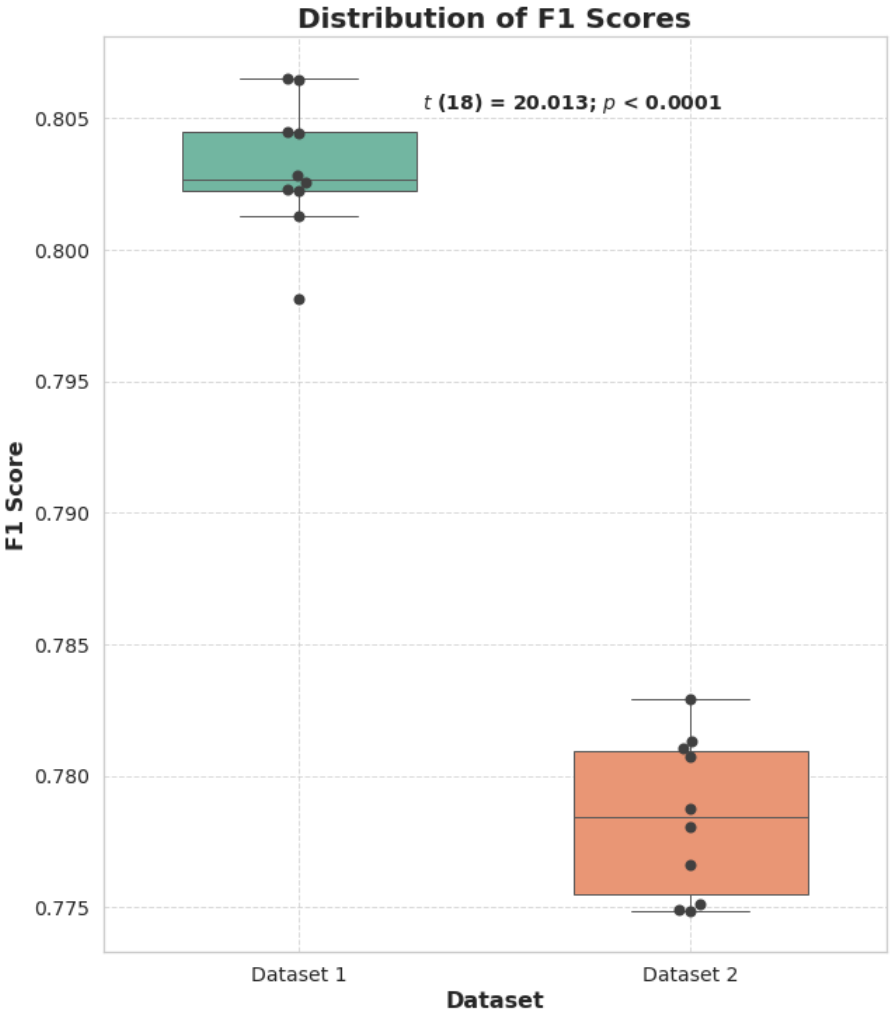

Figure S2: An F1 score comparison between Dataset 1 (doubled dataset using identical images twice with slightly different labels), and Dataset 2 (using only the original dataset with every image appearing once, without label variation).

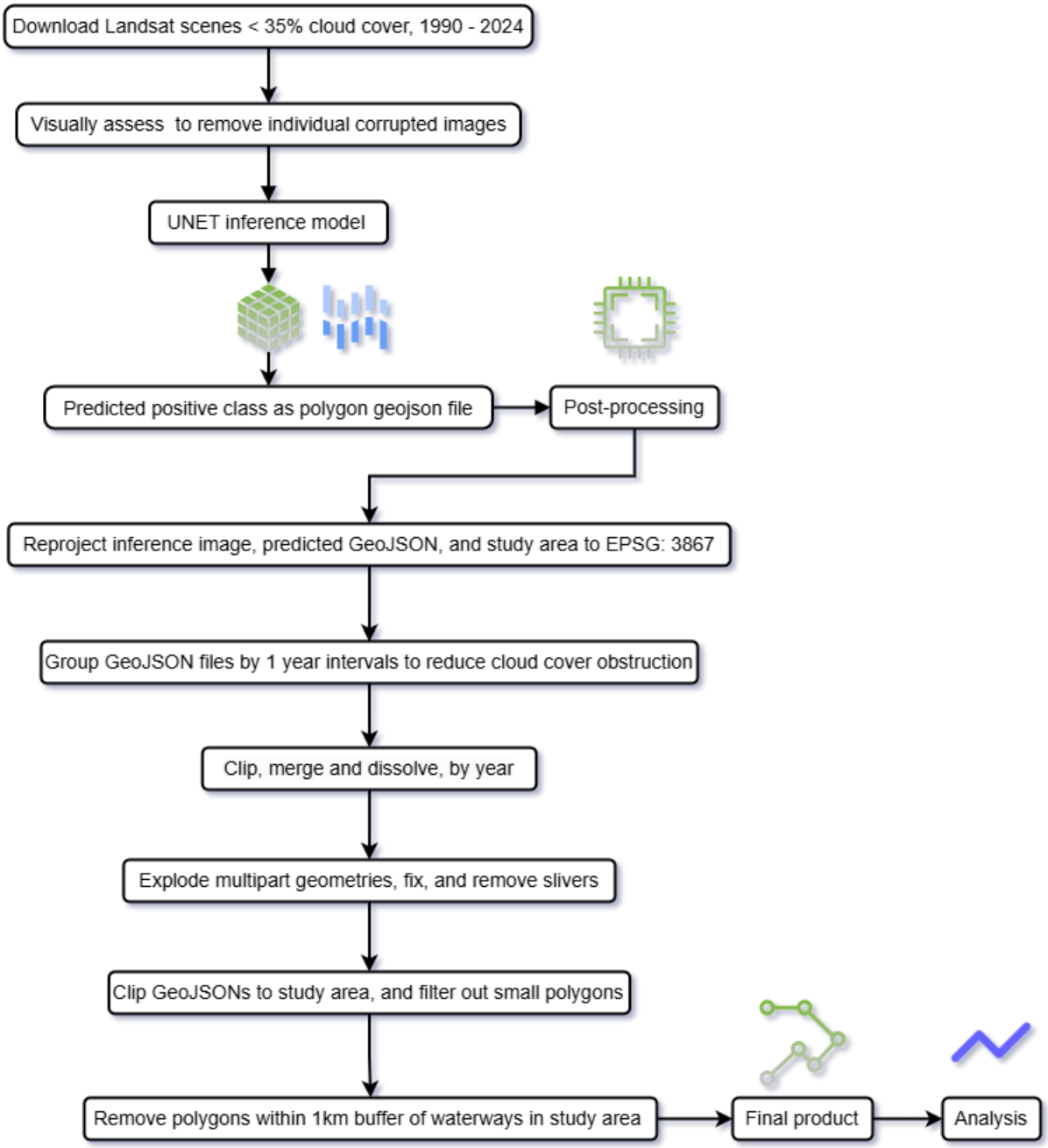

Figure S3: Flow diagram showing the workflow of our model preprocessing, training, model postprocessing, and model polygon output postprocessing before any analysis is performed.

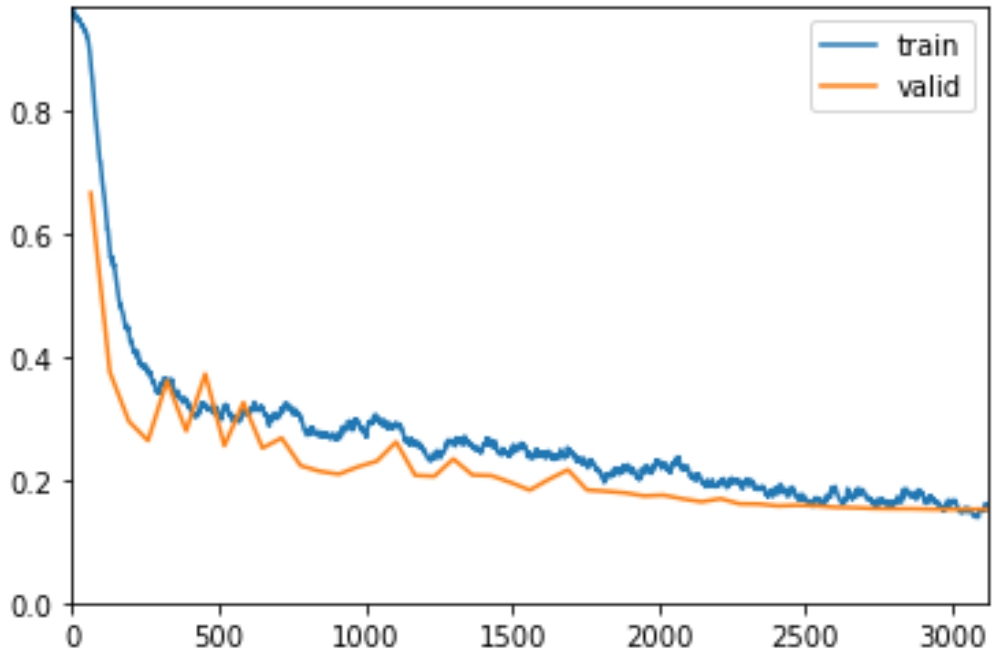

Figure S4: Training (in blue), and validation (in orange) loss curves on a loss plot generated during the training of our final (highest F1) model. The plot shows an ideal outcome where the validation curve stays slightly below the training curve; indicative of the model learning new features and predicting them correctly when tested. The plot also shows the convergence of training and validation curve; indicating that training was stopped at the correct time.

Table S5: Annual count, annual mean area (ha), and annual sum of area (ha) results for all three countries combined.

Year	Count	Mean Area (ha)	Sum of Area (ha)
1995	1235	10.69	13200.00
1996	1459	8.85	12908.12
1997	2383	9.10	21685.93
1998	2095	9.36	19603.04
1999	1914	10.34	19787.20
2000	1956	11.57	22637.51
2001	1656	12.54	20763.22
2002	343	10.38	3558.63
2003	3546	11.32	40134.52

2004	5080	9.85	50028.16
2005	4083	13.32	54394.35
2006	4501	13.68	61558.55
2007	2099	13.32	27968.34
2008	5161	14.10	72765.05
2009	4867	12.61	61379.52
2010	2974	12.38	36806.75
2011	3744	14.05	52585.66
2013	6631	15.55	103098.57
2014	7080	17.04	120643.69
2015	9164	15.79	144709.77
2016	8700	16.88	146893.73
2017	8946	18.35	164176.10
2018	7765	17.98	139580.18
2019	7785	18.13	141134.40
2020	9938	17.73	176224.10
2021	8111	18.52	150204.57
2022	10311	19.67	202767.73
2023	14658	19.07	279460.69
2024	13503	14.77	199489.23

S6: Table of annual count, annual mean area (ha), and annual sum of area (ha) results for Guyana.

Year	Count	Mean Area (ha)	Sum of Area (ha)
1995	782	12.96	10130.98
1996	829	8.76	7262.19
1997	1090	8.56	9327.12
1998	690	12.15	8383.36
1999	747	8.48	6337.89
2000	605	9.85	5959.35
2001	435	7.91	3439.92

2002	91	7.96	724.51
2003	849	11.57	9823.25
2004	1313	10.76	14126.22
2005	1659	12.89	21388.85
2006	1736	12.20	21178.15
2007	419	10.48	4389.81
2008	2231	13.75	30669.66
2009	1195	12.77	15261.69
2010	1109	11.02	12225.02
2011	1654	13.62	22530.85
2013	3951	14.79	58428.09
2014	3871	14.76	57144.62
2015	5764	13.55	78100.09
2016	5019	14.84	74458.52
2017	5496	17.17	94352.50
2018	4390	15.88	69715.57
2019	4298	15.37	66055.37
2020	5595	16.63	93034.20
2021	4629	17.16	79453.45
2022	5655	18.14	102599.46
2023	8752	18.03	157765.23
2024	8175	14.54	118831.71

S7: Table of annual count, annual mean area (ha), and annual sum of area (ha) results for Suriname.

Year	Count	Mean Area (ha)	Sum of Area (ha)
1995	244	6.06	1479.03
1996	275	10.19	2804.26
1997	497	11.95	5941.90
1998	731	8.85	6473.34
1999	576	13.42	7735.12

2000	562	15.07	8472.08
2001	574	18.59	10672.67
2002	212	11.44	2426.54
2003	862	17.32	14931.21
2004	1535	13.06	20061.31
2005	1274	15.30	19500.34
2006	1279	17.05	21812.01
2007	970	15.49	15031.39
2008	1286	19.05	24501.17
2009	1547	18.34	28384.89
2010	1137	14.80	16835.78
2011	1241	17.76	22046.57
2013	1882	19.62	36934.94
2014	2039	24.93	50846.06
2015	2101	26.59	55873.82
2016	2308	26.71	61661.02
2017	2141	26.98	57772.31
2018	2095	28.11	58903.12
2019	2449	26.86	65798.19
2020	2820	24.77	69863.54
2021	2206	27.79	61312.85
2022	2630	30.94	81397.81
2023	2961	32.83	97231.57
2024	3149	21.82	68711.79

887 **Table S8:** Annual count, annual mean area (ha), and annual sum of area (ha)

888 results for French Guiana.

Year	Count	Mean Area (ha)	Sum of Area (ha)
1995	209	7.61	1589.99
1996	355	8.00	2841.67
1997	796	8.06	6416.91
1998	674	7.04	4746.34
1999	591	9.67	5714.19
2000	789	10.40	8206.08
2001	647	10.28	6650.62
2002	40	10.19	407.56
2003	1835	8.38	15380.05
2004	2232	7.10	15840.63
2005	1150	11.74	13505.16
2006	1486	12.50	18568.38
2007	710	12.04	8547.13
2008	1644	10.70	17594.22
2009	2125	8.34	17732.93
2010	728	10.64	7745.95
2011	849	9.43	8008.24
2013	798	9.69	7735.54
2014	1170	10.81	12652.99
2015	1299	8.26	10735.86
2016	1373	7.85	10774.18
2017	1309	9.21	12051.29
2018	1280	8.56	10961.49
2019	1038	8.94	9280.84
2020	1523	8.75	13326.35
2021	1276	7.40	9438.27
2022	2026	9.26	18770.45
2023	2945	8.31	24463.89

2024	2179	5.48	11945.73